

Seismic Retrofit for a Network Arch Bridge with Slit-Type Knock-Off Bearings

Koichi Sugioka

Hanshin Expressway R&D Company Limited, Japan

Nobuhiro Mashima

Hanshin Expressway Company Limited, Japan

Hiroaki Matsushita

Hitachi Zosen Corporation, Japan

Takehiko Himeno

Kawakin Core-Tech Company Limited, Japan

Masahide Matsumura

Osaka City University, Japan



SUMMARY:

Seismic retrofit of an existing network arch bridge against large-scale (Level 2) earthquake ground motions was performed by modifying existing fixed steel bearings into slit-type knock-off bearings. Three-dimensional non-linear dynamic response analyses were carried out considering site-specific ground motions. It was confirmed that shear panel dampers as passive energy-dissipation were needed on both fixed-side and movable-side pier tops to avoid the potentially difficult retrofit work for the undersea pier anchors and foundations. The authors proposed slit-type knock-off bearings with the knock-off function as triggers against the Level 2 earthquake ground motions to provide isolation effect. Performance tests of the slit-type knock-off bearings were conducted to verify the required performance for the seismic retrofit design.

Keywords: Slit-type knock-off bearing, Network arch bridge, Seismic retrofit

1. INTRODUCTION

Seismic response-control has been more commonly applied using seismic response-control devices such as dampers installed in some members or parts that accept damages in the event of large-scale earthquakes but that can be replaced if damaged (e.g. Usami et al., 2006). The seismic response-control would bring significant advantages in the constructions, especially in the seismic retrofit of the existing long-span bridges, with retrofit areas and retrofit members getting smaller which results in construction machines getting smaller and installation space being more effectively used.

The seismic response-control devices have been located between the superstructure and the substructure to decrease or prevent damages in the substructure in the event of severe earthquakes, in terms of effectiveness of energy absorption and accessibility for inspection and replacement of seismic response-control devices. For installing some seismic response-control devices between the superstructure and the substructure at the fixed bearing side, it is needed to make the fixed bearing movable while keeping its fixing function as a fixed bearing at moderate-scale (Level 1) earthquake, as well as to provide some structural members, such as so-called knock off function, to release the fixing function when any horizontal force exceeding the required horizontal force at the Level 1 earthquake is acted and transfer the seismic force to the seismic response-control devices. The authors experimentally studied on the breaking force and the fracture behaviour of the slit-type knock-off structure aiming to propose a new knock off structure meeting the requirements specific to the objective bridge and allow it to properly control its breaking strength complying with the performance requirements.

This study approached from the verification of the current structure by non-linear dynamic response analyses against the Level 2 earthquake ground motions, in the longitudinal direction of the objective steel network arch bridge. Then, retrofit plans by means of a conventional displacement control device and by means of a seismic response-control device were examined to determine the retrofit method. As the result, it was confirmed that a seismic response-control device, a knock off function, were needed to be installed at the fixed bearing side. Finally, a knock off structure to be installed was examined by its full-scale static loading experiment to verify the relationship between the design strength and the breaking strength, the deformation behaviour to a fracture, and the nature of the rupture.

2. SEISMIC RETROFIT WITH SLIT-TYPE KNOCK-OFF BEARING

2.1. Bridge Description

Figure 2.1 shows the network arch bridge located in the Wangan route of the Hanshin Expressway. Its span length is 160 m and arch rise is 30 m. The steel rigid frame piers are supported on rigid caisson foundations embedded in a deep soil stratum. The arch girder is simply supported on pivot bearings (fixed bearing) and pivot roller bearings (moveable bearing).

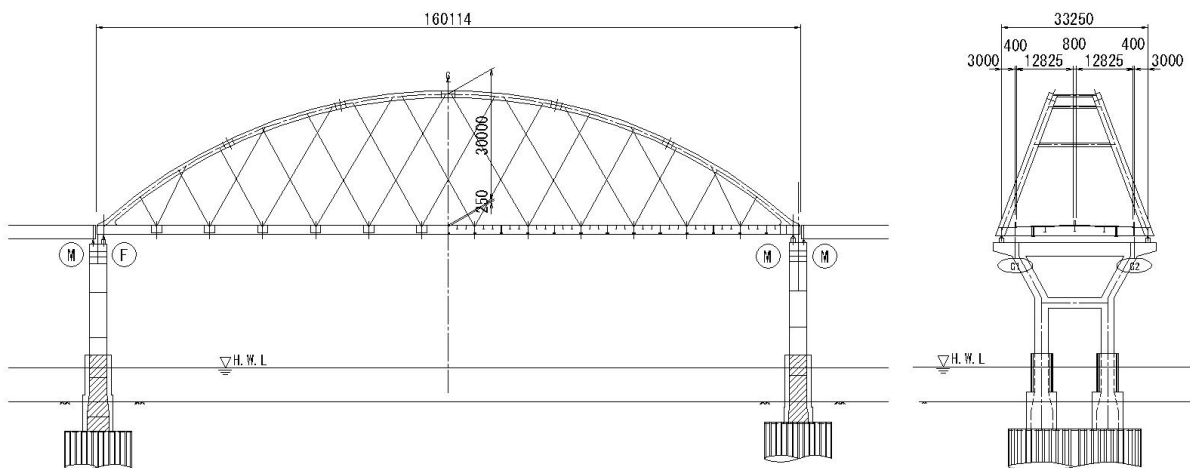


Figure 2.1. General view of arch bridge [unit: mm]

2.2. Seismic Retrofit for the Network Arch Bridge

Three-dimensional non-linear dynamic time history analyses were carried out considering site-specific ground motions. Referring to the seismic design specifications for highway bridges (Japan Road Association, 2002), the whole bridge was modelled using fibre elements. The more detailed information, as well as information on papers not described here for lack of space, was described in the literature (Sugioka et al., 2010). In the current structure, seismic horizontal force about 1.2 times greater than the yield resistance acted on the fixed bearing at the Level 2 earthquake, with a displacement seven times greater than the displacement capacity developed on the movable bearing.

When shear panels as seismic response-control devices were installed only at the movable bearing side, their effect on the decrease in the response values at each part was a little; especially, the response value of the pier foundation at the movable bearing side was not below the ultimate strength. However, with the shear panels installed at both fixed side and movable side, the effect of the shear panels on the decrease in the response value of each part was obtained; the response value of the pier foundation at the movable bearing side was also below the ultimate strength. Therefore, a knock-off structure was needed to be installed at the fixed bearing side.

The characteristic values of the shear panel main body, including the hysteresis curve, were decided referring to the results of the study available in the literature (Sugioka et al., 2011).

2.3. Performance Requirements for Knock-Off Structure

The knock-off structure was needed to release the fixing function against a load exceeding the required horizontal force at the Level 1 earthquake, for which the design rupture yield strength was needed to be set to the value equivalent to the required horizontal force at the Level 1 earthquake. If the actual structure has a actual breaking force lower than the design breaking force, the knock-off members are likely to be frequently replaced every trigger of the knock-off function before generating the horizontal force at the Level 1 earthquake. On the contrary, if the actual breaking force is higher, transfer of load to the shear panels assumed in the analysis would not be performed. Then, the performance requirement for the upper limit of the breaking force of the knock-off structure was needed to be below the yield resistance of the shear panels.

The yield resistance of the shear panels in the literature (Sugioka et al., 2010) was 4,283kN and four shear panels were installed at the fixed bearing side of the pier. Then, the yield resistance per a pier was 17,132kN. The design breaking force required for the knock-off structure of the objective bridge was 10,798kN, which was computed from the horizontal force at the Level 1 earthquake. Therefore, the knock-off member was needed to have the yield strength not less than the required horizontal force at the Level 1 earthquake and also needed to be surely ruptured (fixed support state to be released) by yield strength up to 1.5 ($\cong 17,132/10,798$) times greater than that.

3. SELECTION OF KNOCK-OFF STRUCTURE

As shown in the examples of Figures 3.1 and 3.2, various proposals and researches (e.g. Honjo et al., 2009; Matsumura et al., 2010) were made for the structural types to exert the knock-off function. In the structure focusing on the load working point relatively higher than the rupture part, where a cantilever-beam type side block member was assumed to be used together with a rubber bearing, shown in Figure 3.1, a special slit structure was adopted to suppress the flexural moment onto the rupture section so as to precede the shear fracture. As shown in Figure 3.2, in the structure focusing on the load working point relatively closer to the rupture part where a shear force was likely to dominate, the bolt was notched to control the rupture part. As for these structures, the effectiveness and design method were respectively demonstrated through various loading experiments and analytical studies.

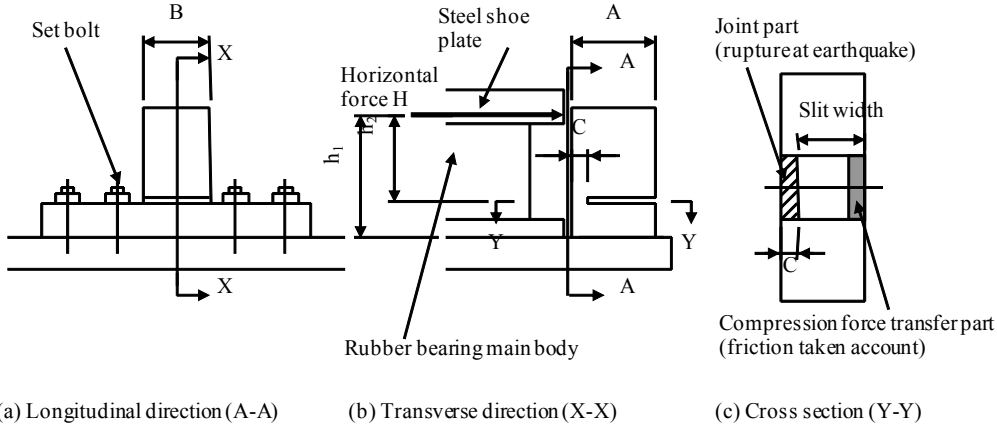


Figure 3.1. Slit-type side block structure (Matsumura et al., 2010)

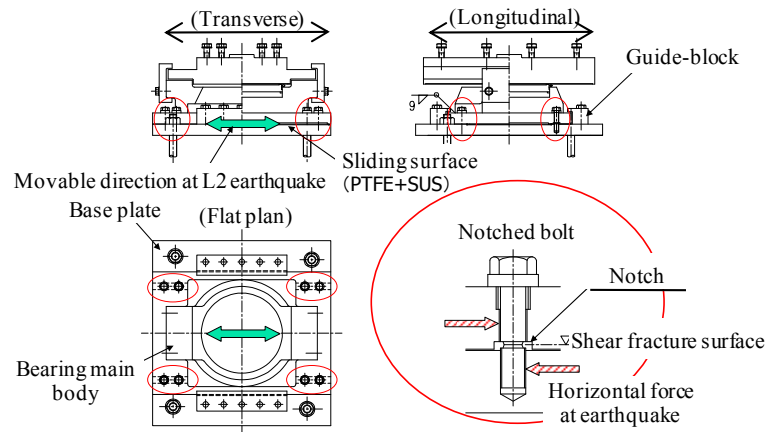


Figure 3.2. Bearing structure with notched bolts (Honjo et al., 2009)

For the objective bridge, however, the replacing work of the existing large pivot bearings, as shown in Figure 3.3, was extremely difficult and therefore the need was a structure that can be installed onto the existing bearing at the site. The authors proposed a new knock-off structure meeting the requirements for this bridge. Figure 3.4 shows the flat plan view of the knock-off structure to be used in the experiment.

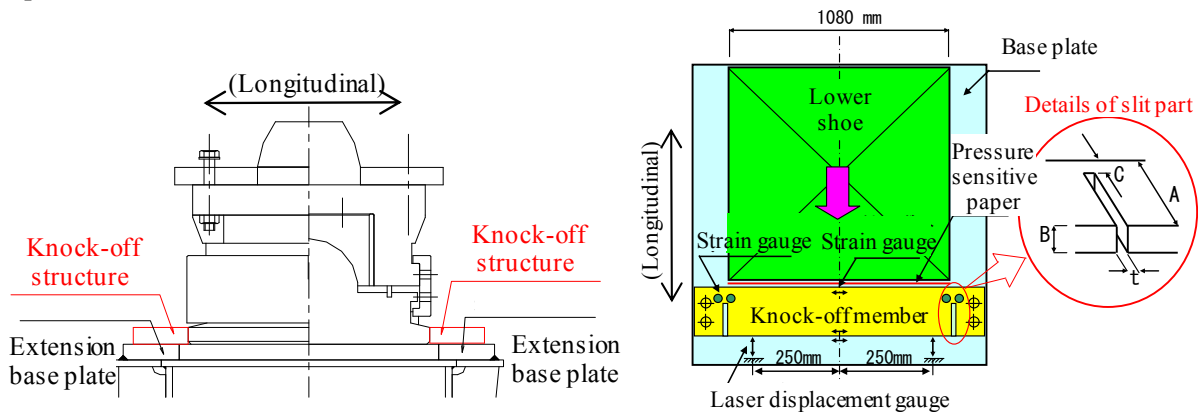


Figure 3.3. Location of knock-off structure

Figure 3.4. Slit-type knock-off structure

The approach to select the knock-off structure selection is described as follows.

- 1) Shear fracture type was selected, rather than a flexural fracture type having different fracture morphology from the ideal one assumed to this bridge because of involving a constant rate of deformation until reaching to the maximum load as well as being difficult to accurately control the rupture yield strength.
- 2) Even against a seismic force corresponding to the Level 1 earthquake, relatively large yield strength was required because these bearings support such large load of about 10,000kN. For this purpose, slit-type structure was focused on, rather than notched-bolt-type structure that would need to install a lot of bolts in larger diameter, if adopted, and would make it difficult to control so as to simultaneously rupture each bolt.
- 3) The original improvements were made based on the fundamental principle of the slit-type structure so as to meet the structural characteristics of a pivot bearing.

4. OUTLINE OF THE EXPERIMENT

The performance validation experiment of the slit-type knock-off bearing focused on the five matters as follows.

- 1) It can be ruptured by a seismic force not less than the required horizontal force at the Level 1 earthquake and yield strength up to 1.5 times greater than that; it was the performance requirement for the bearing structure of the objective bridge.
- 2) To verify the optimization of the geometry of the slits, three different types of the samples were experimented.
- 3) As for the sample with the most effective geometry, another replicate sample was additionally experimented to validate the repeatability of the experimental results.
- 4) The bearing structure at 10,000kN scale assumed for the actual structure was experimented. However, for the safety purpose in the fracture experiment, the thickness of the panel of the knock-off member was reduced than that of the actual structure to decrease the breaking force in the experiment.
- 5) A behaviour close to an ideal shear fracture was desirable to control the knock-off load. For this, in this experiment, the fracture morphology was also considered by measuring the strain distribution under load and observing the fracture surface.

5. EXPERIMENTAL METHOD

5.1. Test specimens

For the experimental samples used to verify the knock-off load and the fracture morphology, total four samples in three different types shown in Table 5.1 were created using SM490 material for all. The sample Case2 having a geometry resulting in the best fracture morphology as described later, the experiment was repeated on the total two replicates to validate the repeatability for individual specificity.

Table 5.1. Dimensions of experimental samples

	Samples (unit)	Knock-off part		Slit part		Slit rate (A-C)/A
		Width	Thickness	Width of rupture part	Slit width	
		A (mm)	B (mm)	C (mm)	t (mm)	
Case1-85%-t3	1	245	60	30	3	0.88
Case2-60%-t3	2	245	18	100	3	0.59
Case3-60%-t10	1	245	18	100	10	0.59

One of the parameters specified for this experiment was a slit rate. This is a ratio of the length of the slit (A-C) to the width (A) of the main body of the knock-off member, as shown in Figure 3.4. When the slit rate is larger, with the width (C) of the rupture part getting relatively smaller, higher shear stress acts. The slit rate was set to about 85% (Case1) proposed as an optimum value referring to the data available in the literatures of studies on side-blocks (Matsumura et al., 2010). However, the slit rate of 60% was also added as an option of the parameter values (Case2 and Case3), which was a desirable value, if applicable, obtained from the results in the design testing conducted taking account of the improvements in the flexibility in design, the availability of installation space, and the workability of the knock-off member on the bridge. The slit width was set to 3mm and 10mm, as a parameter crucial for the morphology of the shear or the flexural failure, to compare these two values.

5.2. Test setup

Bi-axial loading equipment with vertical load capacity up to 24,000kN and 13,000kN horizontal load capacity was used, which was commonly used in the performance test for rubber bearings. The samples were loaded on the horizontal actuator of the equipment.

5.3. Loading method

The loading state is shown in Figure 5.1. The main body of the pivot bearing was modelled with a steel plate to transfer the load to the experimental sample of the knock-off member. The bolt structure was adopted to the part fixing the knock-off member in consideration of the workability at the actual site, and the base plate locating on the bottom of the fixing part was engraved to transfer the shear force to the slits, as shown in Figure 5.2.

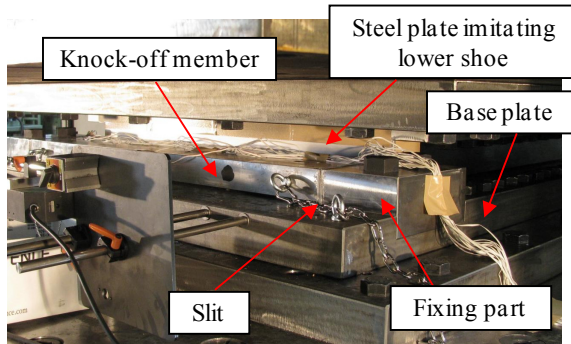


Figure 5.1. Test setup

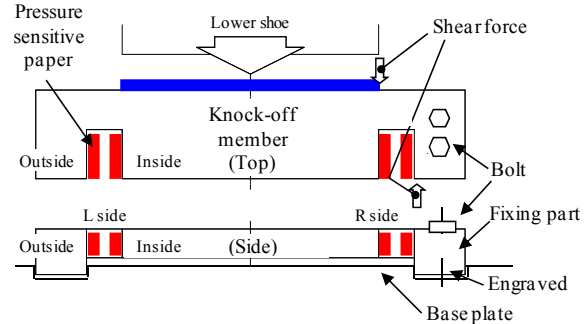


Figure 5.2. Locations of pressure sensitive papers

The loading rate applied to this experiment was at 0.5mm/sec, taking account of the restriction on the capacity of the loading device because the full-scale samples were to be used in the experiment.

A filler plate (Polytetrafluoroethylene or PTFE), which would be applied to the actual structure, was inserted to the gap at the slits to reduce the friction force that might be developed on the slit, referring to the studies available in the literatures (Matsumura et al., 2010).

5.4. Measurement

The horizontal load was detected by the load cell provided on the actuator of the test equipment. The relative displacement between the base plate and the knock-off member, for the horizontal displacement, was directly measured by laser displacement gauges, as shown in Figure 3.4. The contact surface pressure distribution was measured with sensitive papers inserted into the clearance between the lower shoe and the slits together with the filler plate, as shown in Figure 5.2. The principal strain was measured with tri-axial strain gauges attached to know the stress distributions around the slits.

6. RESULTS OF THE EXPERIMENT

6.1. Load-displacement relationship

Load-displacement relationships of the knock-off member samples obtained in the experiment are shown in Figure 6.1. All the samples demonstrated almost the same value in the maximum load (breaking force). According to this result, the authors proposed Equation (6.1) that disregards the term of the friction force in the compression area in the slits developed from the bending moment, modifying the equation recommended by the study available in the literature (Matsumura et al., 2010).

$$H_{\max} = \left(\frac{\sigma_u}{\sqrt{3}} \right) \cdot B \cdot C \quad (6.1)$$

where

H_{\max} : Estimated shear fracture load (N)

- σ_u : Tensile strength of knock-off member (N/mm²)
- B : Thickness of knock-off member in Figure 3.4 (mm)
- C : Width of rupture part of slits in Figure 3.4 (mm)

The breaking force H obtained in the experiment and the design breaking force H_{max} and H'_{max} computed using Equation (6.1) are shown in Table 6.1. H'_{max} was computed by assigning the actual tensile strength of the steel material used in the experiment to the term σ_u in Equation (6.1). When H'_{max} with the actual strength of the material assigned to σ_u was defined as a design value, the actual measurement value H increased by about 15%. When H_{max} with the Japanese Industrial Standards (JIS) upper limit strength of the material assigned to σ_u was defined as a design value, as proposed in this study, it increased by about 10% with respect to the actual measurement value H . Therefore, it was considered that Equation (6.1) was applicable as a design value to be adopted to the actual bridge.

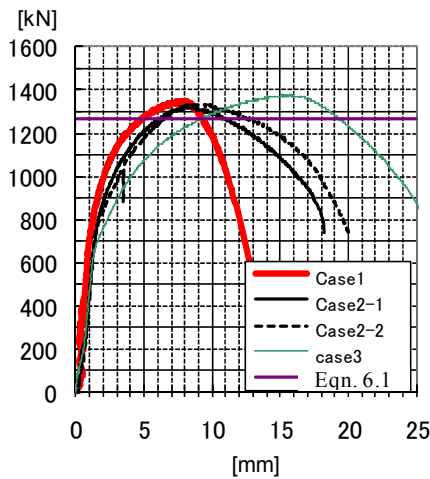


Table 6.1. Breaking force on knock-off members

	Result of experiment Breaking force H (kN)	Design breaking force			
		H _{max} (kN)	H/H _{max}	H' _{max} (kN)	H/H' _{max}
Case1-85%-t3	1350	1268	1.06	1206	1.12
Case2-60%-t3-1	1320		1.04		1.09
Case2-60%-t3-2	1330		1.05		1.10
Case3-60%-t10	1380		1.09		1.14

Figure 6.1. Load-Displacement relationship

Focusing on the displacement behaviour, Case3-60%-t10 with wider slits set to 10mm in width demonstrated a larger displacement 15mm until reaching the maximum load, which was undesirable as a knock-off member to cause other members to serve as a load transfer mechanism after the rupture. Case1-85%-t3 and Case2-60%-t3 with the slit width set to 3mm demonstrate almost the same behaviour regardless of the slit rate.

Therefore, it turns out that the knock-off structure proposed in this paper would adequately control any failure mechanism, even if the slit rate, as an index at which a shear fracture can dominate, decreases from 85% recommended by the studies available in the literatures (Matsumura et al., 2010) to about 60%.

The data obtained from the experiments on the two Case2 replicated to validate the repeatability for individual specificity excellently correspond, only with a little variation.

6.2. Rupture properties

As the results of the experiment shown in Figure 6.2, it was found that the rupture properties of the knock-off member depended on samples. For the Case 3 sample with wider slits, the rupture involved a large flexural deflection. This corresponded with the results in the experiment on the load-displacement relationships mentioned above, where a relatively large deformation was observed until reaching the maximum load, compared to other cases. Moreover, all samples demonstrated the rupture origin at the outside of the root of the slits from which a crack developed toward the inside of the knock-off member main body. With regard to Case1 and Case2 samples different in the slit rate, they demonstrated almost similar behaviours with a small flexural deflection. In this point their fracture morphologies were different from that of Case3.

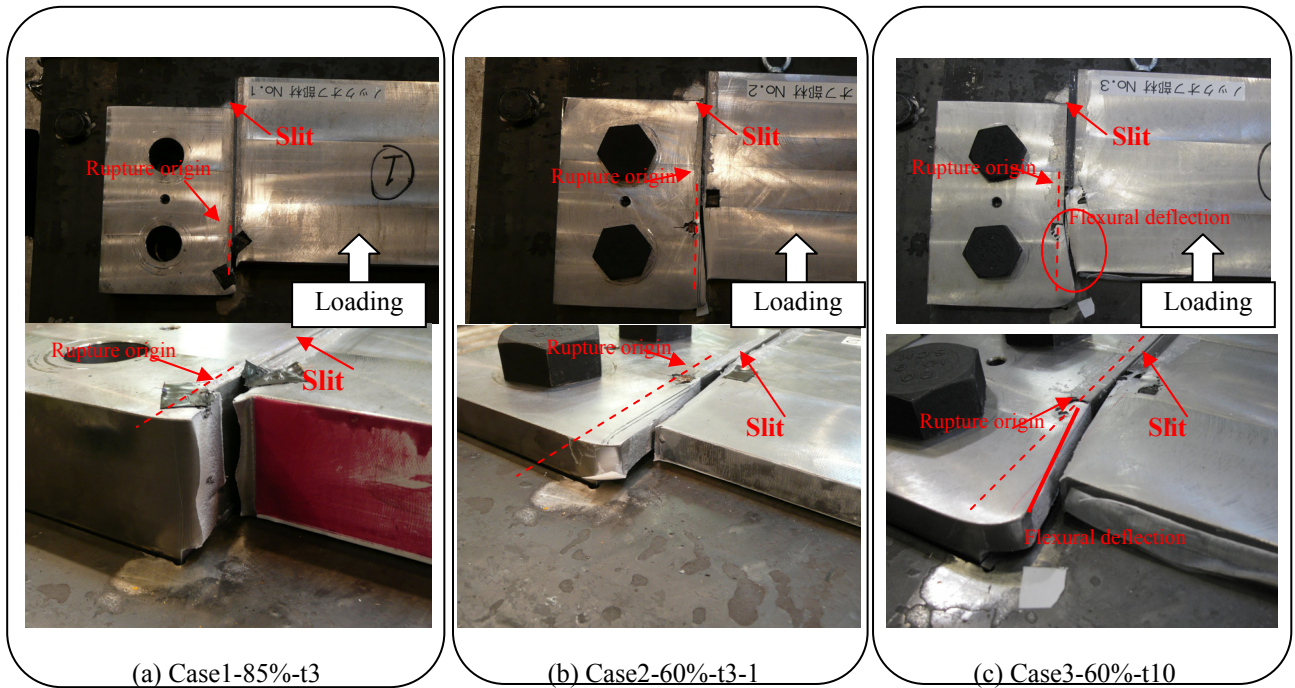


Figure 6.2. Rupture state

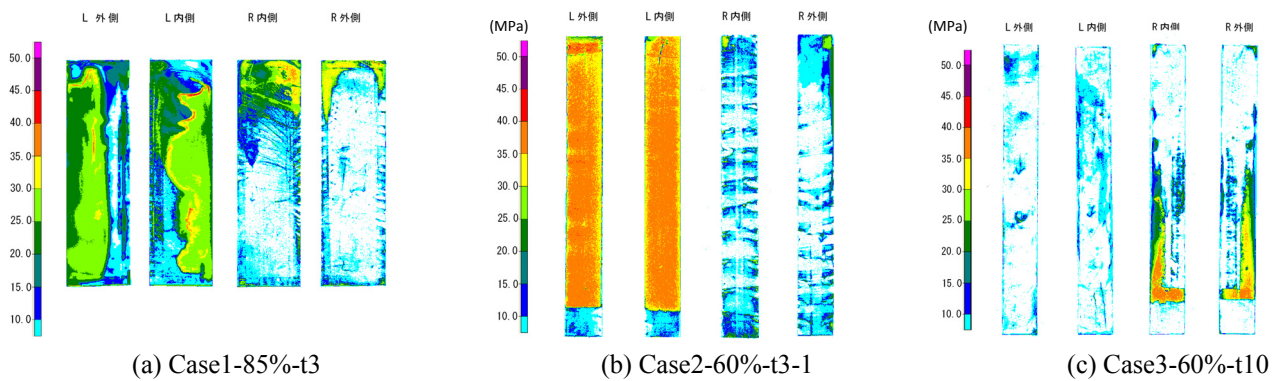


Figure 6.3. Surface pressure distribution around the slit measured by a pressure sensitive paper

Figure 6.3 shows the surface pressure distribution measured by pressure sensitive paper inserted into the slit parts. It can be seen each sample was not always loaded evenly, with different pressure between L side and R side. This corresponded with the actual fracture behaviour where two resistance areas (L side and R side) were ruptured not simultaneously but subsequently one by one on each side.

Moreover, the measured values were 30 to 40 MPa, considerably large, and it was found that a vertical resistance force also acted at the slit parts. It was significant to control the breaking force by suppressing the friction force acting on the slit parts. For this purpose, the PTFE was inserted as a filler plate in this experiment. As the result, it was verified that good correspondence with Equation (6.1) disregarding the influence of friction satisfies a formula to evaluate the breaking force.

6.3. Strain distribution

Figure 6.4 shows the locations of tri-axial strain gauges attached to measure the strain distribution near around the slit parts, as well as the directions of the principal strain around the area with the maximum load; the red arrows show tensile directions. As for the measuring point of the gauge No.2 of the

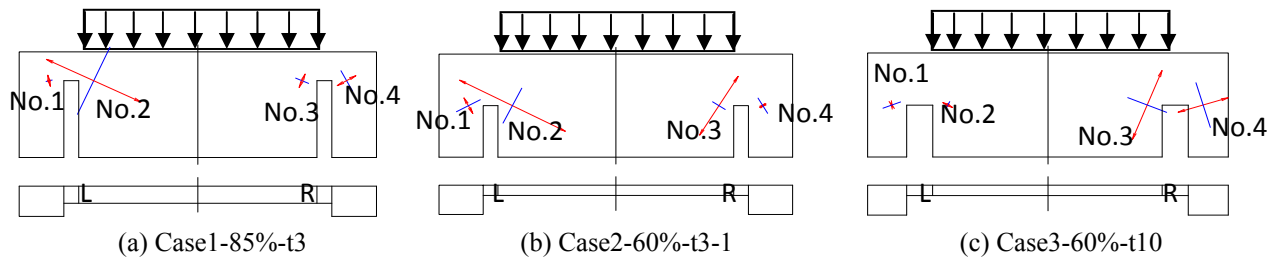


Figure 6.4. Strain distribution (near around max. load)

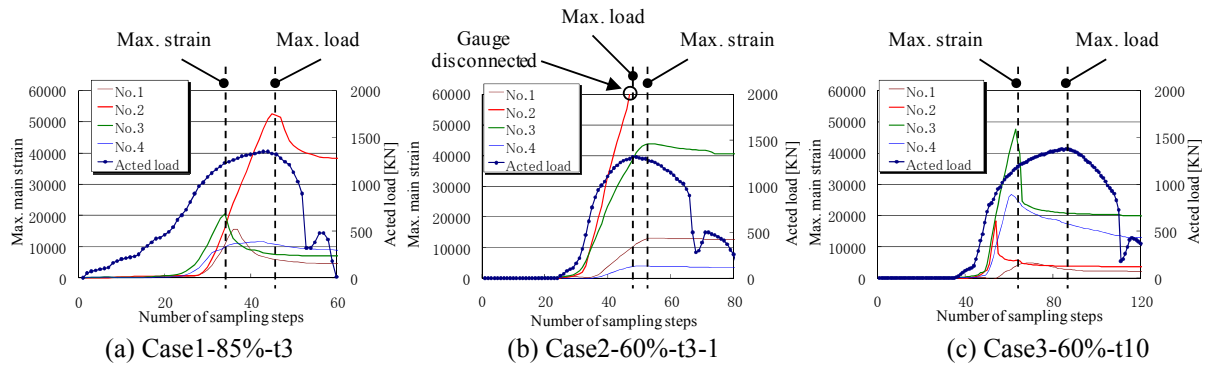


Figure 6.5. Measurement results of main strain

Case2, the measurements were recorded only up to the moment just before reaching the maximum load where the gauge disconnected. Figure 6.5 shows the measurement result of the maximum principal strain at each measuring point along with the load increasing.

The sample Case1 demonstrated a large strain developed at the No.2 measurement point at the knock-off member main unit side. With the largest strain demonstrated at No.2 around at the moment where knock-off member reached the maximum load, no increase of strain was demonstrated at other measurement points. The sample Case2 with a slit rate of 60% demonstrated strains almost evenly developed at the two measurement points (No.2 and No.3) at the knock-off member main body side, with an almost coincidence of the maximum strain and the maximum load developed. The strains were concentrated at the knock-off member main body side and no large strain developed at the fixing member side. Therefore, it was considered that stresses were effectively acted in the area near around the assumed rupture surface.

The sample Case3 with wider slits also demonstrated a large strain developed at No.4 at the fixing member side. This corresponded with the progress of the flexural deflection observed in the experimental results of the rupture properties mentioned above. Almost no strain developed at the slit part on the L side, with a one-sided contact, which can be also evidenced by the strain data. It can be seen that this sample did not demonstrate ideal shear fracture morphology, with a significant difference between the timings of the maximum strain developed and the maximum load developed, resulting in the stress being re-distributed in this case. It was considered to be difficult to allow an assumed structure, if any, to act a load evenly at both slit parts, from the viewpoint of installation errors. However, the breaking forces would be evenly distributed, with no large difference, by re-distribution of the stress before reaching the rupture.

Considering within the range of the data obtained from this experiment, it was found that the design-assumed shear modes were dominant in the samples Case1 and Case2 with a slit width smaller set to 3mm. Therefore, the suitable slit rate would be 60-85% and the slit width would be 3mm for the proposed slit-type knock-off structure.

7. VALIDATION RESULTS FOR THE PERFORMANCE REQUIREMENTS

With regard to the performance requirements for the knock-off structure, it was found that the knock-off structure could control the breaking force up to about 1.1 times greater than the design horizontal force at the required horizontal force at the Level 1 earthquake, as shown in Table 6.1. Furthermore, it might be up to about 1.2 times greater than the design horizontal force, even in consideration of possible 10% increase in the breaking force caused by any influence of dynamic load at earthquake (Matsumura et al., 2010). Thus, the performance requirements were successfully validated for the objective bridge to have a breaking force not less than the required horizontal force at the Level 1 earthquake and also to be broken by a load up to 1.5 times greater than that.

8. CONCLUSIONS

The seismic retrofit of the existing network-arch bridge with slit-type knock-off bearings and also the findings obtained from the validation for the performance of the slit-type knock-off bearings are summarized here.

- 1) With the shear panels installed at both fixed side and movable side, the effect of the shear panels on the decrease in the response value of each part was obtained; the response value of the pier foundation at the movable bearing side was also below the ultimate strength. Therefore, a knock-off structure was needed to be installed at the fixed bearing side.
- 2) As the results of the full-scale experiment for performance validation, the performance requirements of this bridge were verified to be satisfied, according to the proposed design formula for the proposed slit-type knock-off structure.
- 3) It was found that the proposed slit-type knock-off structure would accurately control the rupture properties at the slit rate of 60% with the slit width of 3mm.

REFERENCES

- Honjo, K., Yokoyama, K., Maehara, N., Tasaki, K. and Himeno, T. (2009). Seismic retrofit of existing bridges using a bearing support with knock-off functions. *Journal of Structural Engineering* **55A**, JSCE, 506-514.
- Japan Road Association. (2002). Part V: Seismic Design, Design Specifications of Highway Bridges. Maruzen, Tokyo, Japan
- Matsumura, M., Ochi, N. and Yoshida, M. (2010). Application effect of rupture controllable steel side blocks for viaduct with isolation bearings. *Journal of Structural Engineering* **56A**, JSCE, 554-563.
- Sugioka, K., Kobayashi, H., Mashima, N. and Matsushita, H. (2010). Seismic Retrofit Design for a Network Arch Bridge with Energy Absorbing Devices, *Proceedings of 34th IABSE Symposium on large Structures and Infrastructures for Environmentally Constrained and Urbanised Areas, Venice, Italy, 2010.9*.
- Sugioka, K., Hamada, N., Kobayashi, H., Nishioka, T. and Sugiyama, N. (2011). Experimental study on elastoplasticity characteristics of shear panel dampers for long span bridges. *Journal of Structural Engineering* **57A**, JSCE, 528-541.
- Usami, T. et al. (2006). Guidelines for Seismic and Damage Control Design of Steel Bridges, Edited by Japan Society of Steel Construction (JSSC), Gihodo-Shuppan, Tokyo, Japan